Inorg. Chem. **2008**, *47*, 8278−8285

Stabilization of Plutonium(III) in the Preyssler Polyoxometalate

Mark R. Antonio* and Ming-Hsi Chiang†

Chemical Sciences & Engineering Division, Argonne National Laboratory, 9700 South Cass Avenue, Argonne, Illinois 60439-4831

Received May 15, 2008

The Na^+ ion encapsulated within the Preyssler heteropolyoxoanion, $[NaP_5W_{30}O_{110}]^{14-}$, was exchanged with Pu(III) under hydrothermal conditions to obtain $[Pu(III)P_5W_{30}O_{110}]^{12-}$ (abbreviated $[PuPA]^{12-}$) with hybrid electrochemical properties resulting from the combination of the key redox behaviors of the Pu cation and the P−W−O anion. The electroanalytical chemistry of this two-center, multielectron redox system in a 1 M HCl electrolyte shows that Pu(III) is oxidized to Pu(IV) at the half-wave potential, $E_{1/2}$, of +0.960 V versus Ag/AgCl, which is 0.197 V more positive than the corresponding electrode potential for the Pu(III) aqua ion also in 1 M HCl, indicating the stabilization of the trivalent Pu cation by its encapsulation in the Preyssler polyoxometalate (POM). This effect is uncommon in actinide−POM chemistry, wherein electrode potential shifts of the opposite nature (to more negative values), leading to the stabilization of the tetravalent ions by complexation, are renowned. Moreover, in cyclic voltammetry measurements of the Pu(III) aqua ion and $[PuPA]^{12-}$, the peak currents, i_p, for the one-electron Pu(III)/Pu(IV) processes show different dependencies with the scan rate, ν. The former shows proportionality with $\nu^{1/2}$, indicating freely diffusing species, whereas the latter shows proportionality with ν, indicating a surface-confined one. The first of the five successive two-electron, W-centered reduction processes in $[PuPA]^{12-}$ occurs at $E_{1/2} = -0.117$ V versus Ag/AgCl, which is 1.077 V less than the $E_{1/2}$ for the Pu(III)/Pu(IV) oxidation, thereby providing an experimental, electrochemical measure of the highest occupied molecular orbital/lowest unoccupied molecular orbital energy gap, which compares well with values previously obtained by density-functional theory, complete active space−self consistent field, and post-Hartree−Fock calculations for a series of M^{n+}-exchanged systems, $[MPA]^{n-15}$ for $1 \leq n \leq 4$ (Fernández, J. A.; López, X.; Bo, C.; de Graff, C.; Baerends, E. J.; Poblet, J. M. *J. Am Chem. Soc.* **2007**, *129*, 12244−12253). It was not possible to prepare the Np-exchanged Preyssler anion in the manner of $[PuPA]^{12-}$, because of the instability of tri- and tetravalent Np to oxidation and the formation of the neptunyl(V) ion, which also could not be exchanged for Na^+.

Introduction

The beginnings of *trans*-uranium polyoxometalate (POM) research can be traced to the Russian Academy of Sciences where, in 1976, Saprykin et al. discovered that tetravalent Am and Cm are stabilized by complex formation with the monovacant Wells−Dawson, $[P_2W_{17}O_{61}]^{10-}$, and Keggin, $[PW_{11}O_{39}]^{7-}$, heteropolyoxoanion ligands.[1,2] In their absence, these oxidation states are otherwise reduced to Am(III) and Cm(III) upon contact with water. In 1977, this group further demonstrated that tetravalent Np, Pu, and Cf are also stabilized by complexation with $[P_2W_{17}O_{61}]^{10-}$.[3,4] Since then, a significant amount of research,[5−7] especially that conceived and executed at the Commissariat à l'Energie Atomique,[8−11]

* Author to whom correspondence should be addressed. Fax: +(630) 252 4225. Phone: +(630) 252 9267. E-mail: mantonio@anl.gov.

† Permanent address: Institute of Chemistry, Academia Sinica, 128 Academia Road Sec. 2, Nankang, Taipei 115, Taiwan.

(1) Saprykin, A. S.; Shilov, V. P.; Spitsyn, V. I.; Krot, N. N. *Dokl. Chem., Engl. Transl.* **1976**, *226*, 114–116.

(2) Saprykin, A. S.; Spitsyn, V. I.; Krot, N. N. *Dokl. Phys. Chem., Engl. Transl.* **1976**, *228*, 500–502.

(3) Kosyakov, V. N.; Timofeev, G. A.; Erin, E. A.; Andreev, V. I.; Kopytov, V. V.; Simakin, G. A. *Sov. Radiochem., Engl. Transl.* **1977**, *19*, 418–423.

(4) Kosyakov, V. N.; Timofeev, G. A.; Erin, E. A.; Kopytov, V. V.; Andreev, V. I. *Sov. Radiochem., Engl. Transl.* **1977**, *19*, 66–67.

(5) Termes, S. C.; Pope, M. T. *Trans. Met. Chem.* **1978**, *3*, 103–108.

(6) Kamoshida, M.; Fukasawa, T.; Kawamura, F. *J. Nucl. Sci. Technol.* **1998**, *35*, 185–189.

(7) Yusov, A. B.; Shilov, V. P. *Radiochem., Engl. Transl.* **1999**, *41*, 1–23.

(8) Bion, L.; Moisy, P.; Madic, C. *Radiochim. Acta* **1995**, *69*, 251–7.

(9) Bion, L.; Moisy, P.; Vaufrey, F.; Meot-Reymond, S.; Simoni, E.; Madic, C. *Radiochim. Acta* **1997**, *78*, 73–82.

10.1021/ic8008893 CCC: $40.75
Published on Web 08/12/2008

has demonstrated that tetravalent actinides (An) and lanthanides (Ln) as well (e.g., Pr(IV) and Tb(IV)), which are strong oxidants in the absence of $[P_2W_{17}O_{61}]^{10-}$, are stabilized to spontaneous reduction by complex formation with POMs. The stabilization of the small, tetravalent ions with a high charge-to-radius ratio is manifest by the significant negative shift of electrode potentials for the An(IV)/An(III) and Ln(IV)/Ln(III) redox couples in the complex anions with respect to those for the POM-free aqua cations. For example, in aqueous acid electrolytes, the standard electrode potentials for the Np(IV)/Np(III), Pu(IV)/Pu(III), and Ce(IV)/Ce(III) redox couples of the aqua ions are −0.040, +0.809, and +1.52 V versus Ag/AgCl, respectively.[12] For the same couples in $[Np(IV)(\alpha\text{-}2\text{-}P_2W_{17}O_{61})_2]^{16-}$, $[Pu(IV)(\alpha\text{-}2\text{-}P_2W_{17}O_{61})_2]^{16-}$,[2,13] and $[Ce(III)(\alpha\text{-}2\text{-}P_2W_{17}O_{61})_2]^{17-}$,[14−17] the electrode potentials are shifted in the negative direction by 0.8−1.0 V, indicating that the oxidized, tetravalent states of the f cations are stabilized by POM complexation. It is less common that redox potentials are shifted in the opposite, positive direction,[18] favoring the stabilization of large, trivalent (and divalent) cations by complexation with a polyoxometalate. The metal-exchanged Preyssler heteropolyoxoanions, $[M^{n+}P_5W_{30}O_{110}]^{n-15}$, abbreviated $[M^{n+}PA]^{n-15}$ hereafter, provide examples of such out of the ordinary behaviors for electroactive M ≡ Ce(III),[14,19] Eu(III),[20−22] and, with this report, Pu(III).

Portents of this behavior were provided in the initial studies of M^{n+}-exchange reactions with the as-synthesized Preyssler anion, $[NaP_5W_{30}O_{110}]^{14-}$,[23] in which the Na^+ is incorporated within a tunnel running through the molecular anion,[24−26] see Figure 1. Even under conditions that are known to stabilize Ce(IV), hydrothermal reactions of $H_4Ce(SO_4)_4$ with $[NaPA]^{14-}$ in 1 M aqueous mineral acids, for example, H_2SO_4, result in the exchange of Na^+ with Ce(III) to form $[CePA]^{12-}$.[19] Moreover, it has not proven possible to oxidize Ce(III) in $[CePA]^{12-}$ by electrochemical means within the polarization window available in acidic aqueous electrolytes.[14] In this regard, theory and experiment are in agreement. Very low orbital energies, including an especially exothermic reduction energy, as well as a miniscule highest occupied molecular orbital/lowest unoccupied molecular orbital (HOMO−LUMO) energy gap, were calculated for $[Ce(IV)PA]^{11-}$,[27] all of which are evidence for its instability. In contrast, the corresponding results obtained from density-functional theory and complete active space−self consistent field calculations for $[Ce(III)PA]^{12-}$ are consistent with an energetically stable system in which Ce(III) is nonoxidizable in practice and, accordingly, an experimental value of the formal potential for the Ce(III)/Ce(IV) couple in $[Ce(III)PA]^{12-}$ is not available for comparison with that for the free aqua ion. In line with this preference for the larger and lower charge Ce(III) over Ce(IV), the Preyssler anion was shown to provide a stabilizing environment for Eu(II). X-ray absorption spectroelectrochemistry experiments with $[Eu(III)PA]^{12-}$ show that the one-electron Eu(III) → Eu(II) reduction occurs at a potential that is more positive than the standard electrode potential of −0.55 V versus Ag/AgCl, meaning that Eu(III) incorporated within the tunnel framework of $[EuPA]^{12-}$ is more easily reduced than free Eu(III) in a noncomplexing electrolyte.[20,21,28] Because of significant nonlinear deviations due to correlated electron interactions between the Eu(III)- and W(VI)-centered reductive electrochemistry, the Eu-specific Nernst plot provides only an approximate value of the formal electrode potential—between −0.17 and −0.18 V, which corresponds to values 0.37−0.38 V more positive than the standard electrode potential.[22] The

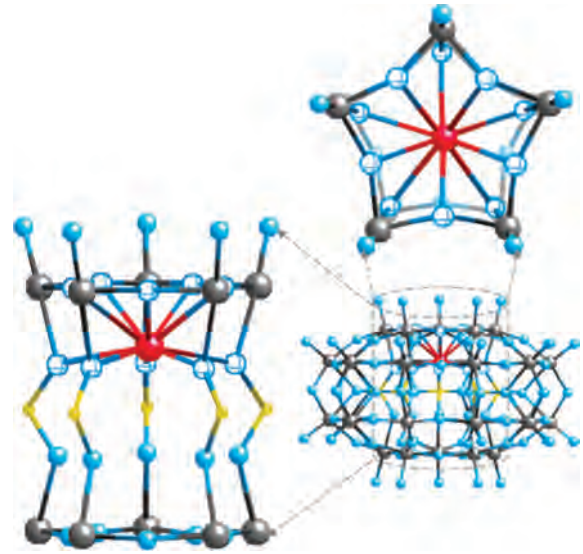

Figure 1. The 145-atom framework structure of the Preyssler anion, $[P_5W_{30}O_{110}]^{15-}$, with its distinctive tunnel that serves to encapsulates M^{n+} cations, shown (bottom right) with O, P, and W as blue, yellow, and gray circles, respectively.[25] The local environment of Pu(III) (red sphere) in $[PuPA]^{12-}$ with its 10 oxygen neighbors, shown as hollow circles in the expanded side (left) and top views (top right) of the tunnel structure, illustrates its siting along the C_5 axis. In these illustrations, the tunnel-encapsulated H_2O molecules are omitted for clarity.

(10) Chartier, D.; Donnet, L.; Adnet, J. M. *Radiochim. Acta* **1998**, *83*, 129–134.
(11) Chartier, D.; Donnet, L.; Adnet, J. M. *Radiochim. Acta* **1999**, *85*, 25–31.
(12) Bratsch, S. G. *J. Phys. Chem. Ref. Data* **1989**, *18*, 1–21.
(13) Chiang, M.-H.; Soderholm, L.; Antonio, M. R. *Eur. J. Inorg. Chem.* **2003**, 2929–2936.
(14) Antonio, M. R.; Soderholm, L.; Williams, C. W.; Ullah, N.; Francesconi, L. C. *J. Chem. Soc., Dalton Trans.* **1999**, 3825–3830.
(15) Ciabrini, J. P.; Contant, R. *J. Chem. Res., Synop.* **1993**, 391.
(16) Haraguchi, N.; Okaue, Y.; Isobe, T.; Matsuda, Y. *Inorg. Chem.* **1994**, *33*, 1015–1020.
(17) Peacock, R. D.; Weakley, T. J. R. *J. Chem. Soc. A* **1971**, 1836–1839.
(18) Ringbom, A.; Wänninen, E. In *Treatise on Analytical Chemistry. Part I: Theory and Practice*, 2nd ed.; Kolthoff, I. M., Elving, P. J., Eds.; J. Wiley & Sons: New York, 1979; Vol. 2, p 441.
(19) Antonio, M. R.; Soderholm, L. *Inorg. Chem.* **1994**, *33*, 5988–5993.
(20) Antonio, M. R.; Soderholm, L. *J. Cluster Sci.* **1996**, *7*, 585–591.
(21) Antonio, M. R.; Soderholm, L. *J. Alloys Compd.* **1997**, *250*, 541–543.
(22) Soderholm, L.; Antonio, M. R.; Skanthakumar, S.; Williams, C. W. *J. Am. Chem. Soc.* **2002**, *124*, 7290–7291.
(23) Creaser, I.; Heckel, M. C.; Neitz, R. J.; Pope, M. T. *Inorg. Chem.* **1993**, *32*, 1573–1578.
(24) Alizadeh, M. H.; Harmalker, S. P.; Jeannin, Y.; Martin-Frere, J.; Pope, M. T. *J. Am. Chem. Soc.* **1985**, *107*, 2662–2669.
(25) Kim, K. C.; Pope, M. T.; Gama, G. J.; Dickman, M. H. *J. Am. Chem. Soc.* **1999**, *121*, 11164–11170.
(26) Dickman, M. H.; Gama, G. J.; Kim, K.-C.; Pope, M. T. *J. Cluster Sci.* **1996**, *7*, 567–583.
(27) Fernandez, J. A.; Lopez, X.; Bo, C.; de Graaft, C.; Baerends, E. J.; Poblet, J. M. *J. Am. Chem. Soc.* **2007**, *129*, 12244–12253.
(28) Soderholm, L.; Liu, G. K.; Muntean, J.; Malinsky, J.; Antonio, M. R. *J. Phys. Chem.* **1995**, *99*, 9611–9616.

driving force for the facile reduction of Eu(III) relates to the stabilizing effects of the coordination environment about Eu(II),[29] which is encapsulated by 10 O atoms within the tunnel-like cavity (see Figure 1), and similar to the stabilization of Eu(II) afforded by its complexation with organic cryptands.[30]

To provide a more quantitative understanding of the redox equilibria and energetics of multivalent metal cations, M^{n+} for $1 \leq n \leq 4$, exchanged into the Preyssler anion, $[M^{n+}P_5W_{30}O_{110}]^{n-15}$, and to complement previous research with the 4f-element-exchanged anions, our efforts turned to the preparation of *trans*-uranium, 5f-element-exchanged ones. In view of the renown intricacies and complexities of the aqueous redox chemistry of Np and Pu in particular—wherein oxidation states can vary from III to VII and their relative stabilities toward disproportionation and hydrolysis reactions are strongly affected by pH and the presence of complexing ligands[31,32] —we thought it of particular interest to study their interactions with the Preyssler anion. In terms of 5f-element-exchange chemistry, thus far it has only been possible to characterize the Th(IV)-, U(IV)-, Am(III)-, and Cm(III)-encapsulated Preyssler anions, which have been obtained from simple exchange reactions with $[NaPA]^{14-}$ in acidic aqueous media.[23,26,33] We describe the preparation and optical and electrochemical characterization of $[Pu(III)P_5W_{30}O_{110}]^{12-}$ and comment upon preparative failures with the Np analog. The measured electrochemical energy gap of the heterobinuclear $[PuPA]^{12-}$ complex anion is shown to compare favorably with the calculated frontier orbital energies for other $[M^{n+}PA]^{n-15}$ systems[27,34] despite the intrinsic disparity with experimental results wherein, from the theoretical viewpoint, the HOMO−LUMO gap is estimated by the difference between the electron affinity and ionization potential energies, whereas the electrochemical value is obtained as the difference between the applied electrode potentials for the first reduction and the first oxidation.

Experimental Section

Sample Preparation. ***Caution!*** *The radioactive isotopes ^{237}Np and ^{242}Pu pose serious health risks due to the emission of ionizing radiation and should be handled only in controlled laboratory facilities with the appropriate environment, safety, and health infrastructure.* The Preyssler salt, $K_{12.5}Na_{1.5}[NaP_5W_{30}O_{110}]\cdot 15H_2O$, was obtained by hydrothermal means as described elsewhere[23] and was subsequently subjected to hydrothermal reactions with ^{242}Pu and ^{237}Np in order to ion-exchange Na^+ in $[NaPA]^{14-}$, as described below.

a. $K_{12}[PuP_5W_{30}O_{110}]\cdot nH_2O$. The $K_{12.5}Na_{1.5}[NaPA]\cdot 15H_2O$ salt (0.081 g) was dissolved in 1 mL of 0.05 M HCl to make a clear and colorless 9.8 mM solution of $[NaPA]^{14-}$, which was contained in a threaded perfluoroalkoxy (PFA) vial (Savillex No. 201-007-10-024-01). An approximately 2× molar excess of Pu, in the form of a redox-pure pale-green stock solution of 0.02 M Pu(IV) in 1 M HNO_3 as prepared by standard methods of previous description,[35] was injected (1 mL, equivalent to nearly 0.005 g of ^{242}Pu) into the $[NaPA]^{14-}$ solution with stirring to produce a pale-green solution with some green precipitate. The vial was sealed with its matching PFA threaded closure and placed in the polytetrafluoroethylene (PTFE) cup of a large-capacity acid digestion bomb (Parr No. 4748) to which water was added to half-fill the cup. The entire double-boiler assembly was sealed shut and placed in a crucible furnace at 190 °C for 25 h. Upon cooling, the inner PFA vial was found to contain a brown liquor and a green precipitate, whose appearance was noted before the hydrothermal treatment. To screen for an indication of a successful ion-exchange reaction, the liquor was subjected to optical spectroscopy as well as cyclic voltammetry (CV), both of which revealed the absence of the Pu(IV) and $[NaPA]^{14-}$ reactants, and on the basis of that evidence, the solution was worked-up as follows. The precipitate was removed by centrifugation. Excess KCl was added to the isolated mother liquor to produce a drab-looking precipitate, which was centrifuged to facilitate separation from the liquid. The isolated precipitate was redissolved in fresh H_2O (2 mL) and reprecipitated with excess KCl. This workup was repeated four times to rid the product of any adventitious Pu and provided a quantitative yield of a peach-color solid, $[Pu(III)PA]^{12-}$, based upon $[NaPA]^{14-}$.

b. Reaction of Np(IV) with $[NaP_5W_{30}O_{110}]^{14-}$. In a typical reaction, the $K_{12.5}Na_{1.5}[NaPA]\cdot 15H_2O$ salt (0.13 g) was dissolved in 1.6 mL of 0.025 M H_2SO_4 to make a clear, colorless 9.9 mM solution of $[NaPA]^{14-}$, which was contained in a threaded Savillex PFA vial. A 12% molar excess of Np, in the form of a redox-pure pale-green stock solution of 0.016 M Np(IV) in 1 M $HClO_4$, as prepared by standard methods of previous description,[36] was injected (1.1 mL, equivalent to 0.004 g of ^{237}Np) into the $[NaPA]^{14-}$ solution with stirring to produce a pale-green solution free of precipitate. The vial was sealed, placed in the PTFE cup of a Parr bomb, and heated as described in section a above, after which the primary PFA vial was found to contain a clear pale-green solution without precipitate. This solution was subjected to screening through the use of optical spectroscopy, which showed the presence of neptunyl(V) by the characteristic 980 nm band,[32] as well as cyclic voltammetry, which revealed the presence of the parent $[NaPA]^{14-}$ anion, see the Supporting Information, Figure 1. Despite repeated attempts with variations of H_2SO_4 concentrations from 0.025 to 1 M, Na^+ in $[NaPA]^{14-}$ could not be exchanged for neptunium by the methods employed here.

Instrumentation and Characterization

Optical spectra were obtained in 1-cm-path-length quartz cells by use of an Olis-converted Cary-14 spectrophotometer. A BAS 100B/W potentiostat was used for the acquisition of all CV data, which were obtained at room temperature in a 1 M HCl electrolyte (Optima, Fisher Chemical) in single-compartment glass cell vials using a standard three-electrode system consisting of 3.05 mm diameter graphite rod working and auxiliary electrodes (Alfa

(29) Chiang, M.-H.; Antonio, M. R.; Williams, C. W.; Soderholm, L. *Dalton Trans.* **2004**, 801–806.
(30) Yee, E. L.; Gansow, O. A.; Weaver, M. J. *J. Am. Chem. Soc.* **1980**, *102*, 2278–2285.
(31) Clark, D. L.; Hecker, S. S.; Jarvinen, G. D.; Neu, M. P. In *The Chemistry of the Actinide and Transactinide Elements*; Morss, L. R., Edelstein, N. M., Fuger, J., Eds.; Springer: Dordrecht, The Netherlands, 2006; Vol. *2*, pp 813−1264.
(32) Yoshida, Z.; Johnson, S. G.; Kimura, T.; Krsul, J. R. In *The Chemistry of the Actinide and Transactinide Elements*; Morss, L. R., Edelstein, N. M., Fuger, J., Eds.; Springer: Dordrecht, The Netherlands, 2006; Vol. *2*, pp 699−812.
(33) Antonio, M. R.; Williams, C. W.; Soderholm, L. *J. Alloys Compd.* **1998**, *271*−*273*, 846–849.
(34) López, X.; Fernandez, J. A.; Poblet, J. M. *Dalton Trans.* **2006**, 1162–1167.
(35) Wilson, R. E.; Hu, Y. J.; Nitsche, H. *Radiochim. Acta* **2005**, *93*, 203–206.
(36) Antonio, M. R.; Soderholm, L.; Williams, C. W.; Blaudeau, J.-P.; Bursten, B. E. *Radiochim. Acta* **2001**, *89*, 17–25.

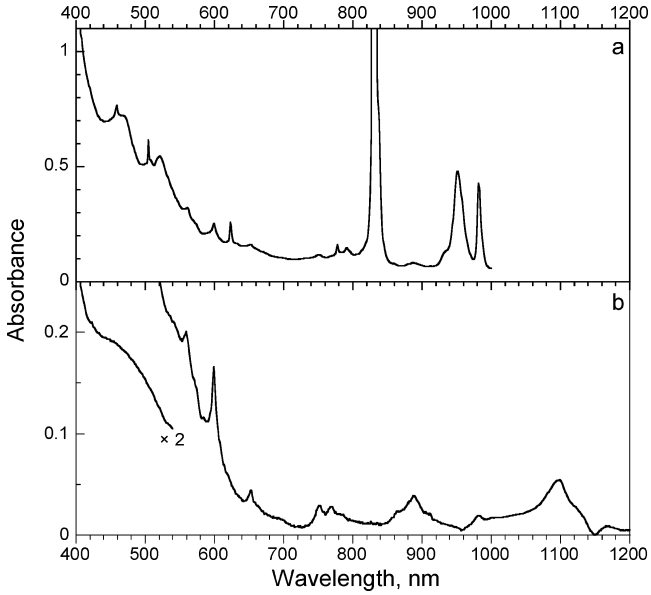

Figure 2. Optical spectra of (a) mother liquor resulting from the hydrothermal ion-exchange reaction of Pu(IV) with $[NaPA]^{14-}$ and (b) purified Pu-exchange product in 1 M HCl.

40765), and Ag/AgCl reference electrodes (BASi MF-2052), against which all electrode potentials are reported herein. The cyclic voltammograms were acquired with repetitive sweeps, which were started at the electrode rest potential (+0.69 V) and with a negative initial scan direction.

Results

The optical spectrum for the mother liquor obtained from the hydrothermal reaction of Pu(IV) with $[NaPA]^{14-}$ is shown in Figure 2a. All of the strong principal features, especially the intense band at 830 nm, are readily attributed to the plutonyl(VI) ion, and the weaker ones are suggestive of Pu(III).[31] The spectrum for the solution of the purified solid of $[Pu^{n+}PA]^{n-15}$ (9 mM in 1 M HCl) is shown in Figure 2b. The plutonyl(VI) response is gone, and the absorption is characterized by a series of slight and generally broad features. The bands at 599, 653, and 1099 nm are reminiscent of the response of the Pu(III) aqua ion, but the last two may be consistent with the Pu(IV) aqua ion as well. An unambiguous assignment of the Pu oxidation state, n^+, in $[Pu^{n+}PA]^{n-15}$ is not possible from the visible-NIR spectrum of Figure 2b. In this regard, electroanalytical data provide conclusive insight because previous research has shown that the charge of the encapsulated ion has a strong influence on the electronic properties of the LUMO states, which are of essentially W 5d-orbital character, and, hence, on the voltammetric response.[23,27,28,33,37,38]

The cyclic voltammogram obtained for a 2.5 mM solution of $[PuPA]^{n-15}$ in the 1.70 V polarization window afforded by the 1 M HCl electrolyte is shown in Figure 3. There are five well-resolved couples between 0.0 and −0.6 V (identified as I−V), and one couple between +0.9 and +1.0 V (identified as I′). From previous accounts of electroanalytical

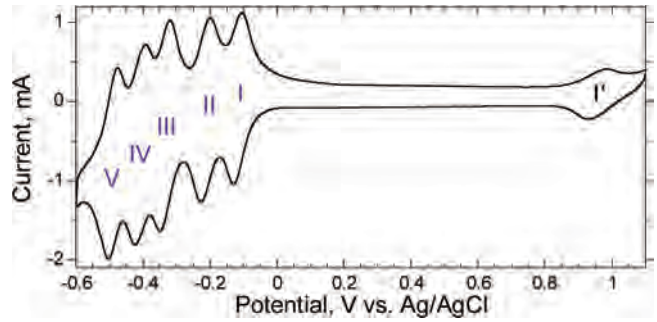

Figure 3. Cyclic voltammogram of the purified Pu-exchange product obtained in 1 M HCl, $\nu = 50$ mV s^{-1}, over a wide polarization window, −0.6 to +1.1 V, that shows the five successive two-electron redox waves (identified as I−V) of the W−O framework structure at negative electrode potentials that are diagnostic of trivalent Pu encapsulation and the one-electron wave (identified as I′) of the Pu(III)/Pu(IV) redox couple at positive electrode potentials.

characterizations of an extensive series of $[M^{n+}PA]^{n-15}$ incorporating mono-, di-, tri-, and tetravalent M cations,[33,38] the response shown here at negative electrode potentials is typical of that seen for M^{3+} exchange with Na^+ in the Preyssler anion. The changes in the W-based electrochemistry of $[M^{n+}PA]^{n-15}$ at negative electrode potentials with different M^{n+}'s are clear-cut and permit us to assign the plutonium valence as trivalent in the as-synthesized complex, $[Pu(III)PA]^{12-}$. It follows, that the redox couple with the measured half-wave potential, $E_{1/2}$, of +0.960 V is due to the Pu(III)/Pu(IV) process. Table 1 contains all of the conventional electrochemical parameters for $[PuPA]^{12-}$ obtained from the CV measurements.

Figure 4a illustrates the effects of scan rate, ν (for 10, 25, 50, and 100 mV s^{-1}), on the CV data for the five W-based redox couples (I−V). Information about the kinetics of electron transfer for each of these processes is provided by plots of the peak currents for the anodic and cathodic waves (i_{pa} and i_{pc}, respectively) versus the square roots of the scan rates, $\nu^{1/2}$. Figure 4b shows that a direct proportionality exists between the currents and $\nu^{1/2}$. The primary data (shown as symbols) are adequately described by the linear fits ($R^2 = 0.977-0.999$, shown as lines) with intercepts of zero according to the Randles−Sevcik equation,[39] $i_p = (nF)^{3/2}\nu^{1/2}ACD^{1/2}(5.02RT)^{-1/2}$ with the conventional symbol meanings,[40] indicating that the electron transfer kinetics are mass-transport-controlled. The individual slopes and regression coefficients, provided in Table 2, show that the ratios of the average peak currents, i_{pa}/i_{pc}, vary about unity by ±5% for all five waves for $10 \leq \nu \leq 100$ mV s^{-1} (see the Supporting Information, Figure 2), indicating ideal (reversible) behaviors free from complications associated with the reactivity of the electrolyzed anion. The separation of peak potentials, $\Delta E_p = E_{pa} - E_{pc}$, for couples I−V exhibits a mild dependence on the scan rate (see the Supporting Information, Figure 3), with average values of 23−29 mV that are consistent with five

(37) Capdevila, H.; Vitorge, P. *Radiochim. Acta* **1995**, *68*, 51–62.
(38) Chiang, M. H.; Antonio, M. R.; Soderholm, L. *Dalton Trans.* **2004**, 3562–3567.
(39) Heineman W. R.; Kissinger, P. T. In *Laboratory Techniques in Electroanalytical Chemistry*, 2nd ed.; Kissinger, P. T., Heineman, W. R., Eds.; Marcel Dekker: New York, 1996, pp 51−125.
(40) Bard, A. J.; Faulkner, L. R. *Electrochemical Methods: Fundamentals and Applications*, 2nd ed.; John Wiley & Sons: New York, 2001.

Table 1. Half-Wave Potentials, $E_{1/2}$ (±5 mV),[a] and Peak Separations, ΔE_p in millivolts,[b] for the Redox Couples Observed in the Cyclic Voltammograms of Figures 4a and 5 for $[Pu(III)P_5W_{30}O_{110}]^{12-}$ and the Pu(III) Aqua Ion in 1 M HCl for Four Different Scan Rates, ν in millivolts per second, on GR Working Electrodes

	tungsten waves										Pu waves	
	I		II		III		IV		V		I′	
ν	$E_{1/2}$	ΔE_p	$E_{1/2}$	ΔE_p	$E_{1/2}$	ΔE_p	$E_{1/2}$	ΔE_p	$E_{1/2}$	ΔE_p	$E_{1/2}$	ΔE_p
						$[Pu(III)PA]^{12-}$						
10	−116	16	−213	22	−334	24	−405	22	−487	22	+961	35
25	−117	22	−212	24	−334	28	−407	26	−489	22	+960	49
50	−117	26	−212	28	−334	32	−407	30	−489	30	+959	74
100	−116	28	−214	32	−334	36	−408	36	−492	32	+960	103
avg.	−117	23	−213	27	−334	29	−407	29	−489	27	+960	65
						Pu(III) Aqua Ion						
16											+762	60
25											+763	63
49											+762	64
100											+763	70
avg.											+763	64

[a] $E_{1/2} = (E_{pc} + E_{pa})/2$, where E_{pa} is the electrode potential of peaks with anodic current and E_{pc} is the electrode potential of peaks with cathodic current. [b] $\Delta E_p = E_{pa} - E_{pc}$.

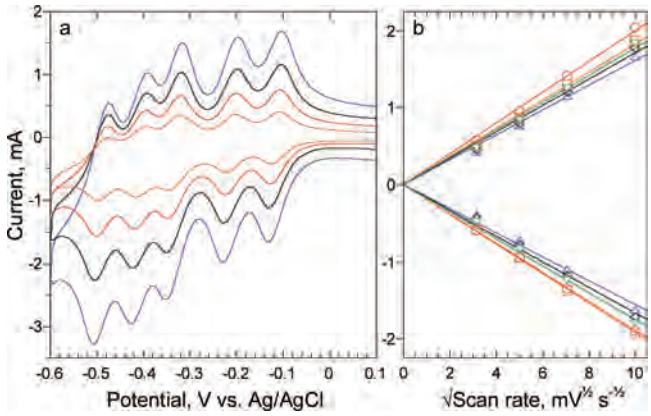

Figure 4. (a) Cyclic voltammograms of $[PuPA]^{12-}$ obtained at scan rates of 10, 25, 50, and 100 mV s^{-1} (orange, red, black, and blue lines, respectively) in a narrow electrode polarization region showing the W-based electrochemical behavior at negative electrode potentials. (b) Anodic and cathodic peak current, i_{pa} and i_{pc}, variations of the five couples with the square roots of scan rates from the voltammograms of a. The fitted lines to the experimental data (shown as symbols with blue triangles, black diamonds, red circles, orange squares, and green inverted triangles for waves I, II, III, IV, and V, respectively) are based upon the Randles−Sevcik equation, see the text. All slopes, which are negative for the i_{pc} response and positive for i_{pa}, and regression coefficients are provided in Table 2.

Table 2. Slopes and Regression Coefficients of Linear Least Squares Fits to i_{pc} and i_{pa} versus Square Root of Scan Rate, $\nu^{1/2}$, for W-Based Redox Couples I−V of $[PuPA]^{12-}$ (Shown in Figure 4b) and for the Pu(III)/Pu(IV) Redox Couple (I′) of the Pu(III) Aqua Ion (Shown in Figure 6b)[a]

wave	slope, i_{pa}[b]	R^2[c]	slope, i_{pc}[d]	R^2[c]	$\lvert i_{pa}/i_{pc}\rvert$[e]
			Tungsten Couples		
I	+0.162(4)	0.9871	−0.156(6)	0.9771	1.04
II	+0.172(5)	0.9850	−0.167(5)	0.9852	1.03
III	+0.200(4)	0.9939	−0.190(1)	0.9997	1.05
IV	+0.183(4)	0.9913	−0.192(2)	0.9989	0.95
V	+0.178(5)	0.9870	−0.175(4)	0.9895	1.02
			Plutonium Couples		
I′, $[PuPA]^{12-}$	+0.0076(3)	0.9845	−0.0070(1)	0.9979	1.09
I′, Pu(III)	+1.77(2)	0.9970	−1.37(2)	0.9966	1.29

[a] The i_{pc} and i_{pa} data for the Pu(III)/Pu(IV) redox couple (I′) of $[Pu(III)PA]^{12-}$ (shown in Figure 6a) are best modeled with linear least squares fits dependent upon ν, in contrast to the $\nu^{1/2}$ proportionality for the Pu(III) aqua ion. [b] i_{pa} is the peak anodic current, and the slope is given as $mA \cdot s^{1/2} \cdot mV^{-1/2}$ except for couple I′ of $[PuPA]^{12-}$, which is in $mA \cdot s \cdot mV^{-1}$. [c] Regression coefficients for fits to data with the Randles−Sevcik equation, except for couple I′ of $[PuPA]^{12-}$, which was fit with an adsorption model. [d] i_{pc} is the peak cathodic current, and the slope is given as $mA \cdot s^{1/2} \cdot mV^{-1/2}$ except for couple I′ of $[PuPA]^{12-}$, which is in $mA \cdot s \cdot mV^{-1}$. [e] This quotient represents the average value for the four scan rates 10, 25, 50, and 100 mV s^{-1} for $[PuPA]^{12-}$ and 16, 25, 49, and 100 mV s^{-1} for the Pu(III) aqua ion.

successive two-electron process at 25 °C, in agreement with the known reductive electrochemistry of $[M^{3+}PA]^{12-}$.[23,33,38]

The cyclic voltammograms of Figure 5 focus on the Pu-centered electrochemistry of $[Pu(III)PA]^{12-}$ and, for comparison, the Pu(III) aqua ion in the polarization window between +0.6 and +1.1 V at four different scan rates. The average $E_{1/2}$ value for $[PuPA]^{12-}$ is +0.960 V, see Table 1. That for the aqua ion is +0.763 V, which is in agreement with previous measurements of the Pu(III)/Pu(IV) formal electrode potential in 1 M hydrochloric acid electrolytes[37,41] and for which the standard electrode potential is +0.806 V in acid solution.[12] Of particular mention here is the nearly 0.20 V greater value of $E_{1/2}$ for $[PuPA]^{12-}$ than for the Pu(III) aqua ion. Plots of the peak current dependencies on the scan rate are shown in Figure 6a and b for $[Pu(III)PA]^{12-}$ and the Pu(III) aqua ion, respectively. Whereas i_{pa} and i_{pc} for the Pu(III)/Pu(IV) couple of the aqua ion exhibit linearity with $\nu^{1/2}$ and a zero intercept ($R^2 = 0.997$, see Table 2), as expected for nernstian waves of diffusing species,[39,40] the corresponding data for $[Pu(III)PA]^{12-}$ exhibit linearity with ν and a zero intercept ($R^2 = 0.984-0.994$, see Table 2). This behavior suggests a nernstian, surface-confined redox process,[39,40] according to $i_p = (nF)^2 \nu AT(4RT)^{-1}$. Fitting the Pu response, I′, for $[PuPA]^{12-}$ to the mass-transport-controlled model with $\nu^{1/2}$ dependence results in substandard correspondence to the experimental data (see the Supporting Information, Figure 4a) and lower values of R^2, 0.809−0.869. Similarly, fitting the response for the Pu(III) aqua ion to the surface-controlled model with ν dependence results in substandard correspondence to the experimental data (see the Supporting Information, Figure 4b) and lower values of R^2, 0.225−0.497. For the Pu wave of $[PuPA]^{12-}$, the average $\lvert i_{pa}/i_{pc}\rvert$ ratio is ca. 10% greater than unity for $10 \leq \nu \leq 100$ mV s^{-1} (see Table 2 and the Supporting Information,

(41) Rabideau, S. W.; Cowan, H. D. *J. Am. Chem. Soc.* **1955**, *77*, 6145–6148.

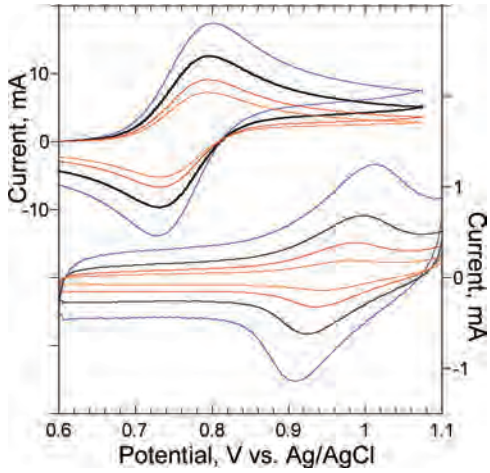

Figure 5. Cyclic voltammograms of $[PuPA]^{12-}$ obtained at scan rates of 10, 25, 50, and 100 mV s^{-1} (orange, red, black, and blue lines, respectively, on bottom) and for the Pu(III) aqua ion obtained at scan rates of 16, 25, 49, and 100 mV s^{-1} (orange, red, black, and blue lines, respectively, on top) in a narrow electrode polarization region showing the Pu-based electrochemical behavior at positive electrode potentials.

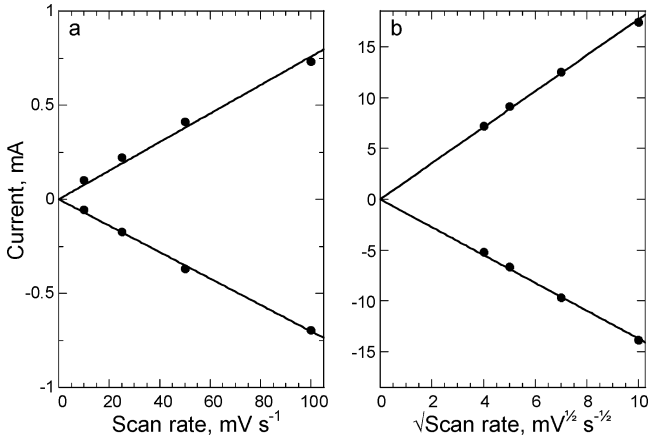

Figure 6. Anodic and cathodic peak current, i_{pa} and i_{pc}, variations of the Pu redox couples (I′) with variations of scan rates from the voltammograms of Figure 5. (a) The fitted lines to the experimental data (circles) of $[PuPA]^{12-}$ are based upon the direct proportionality of i_p with ν, according to the surface confinement model. All slopes, which are negative for the i_{pc} response and positive for i_{pa}, and regression coefficients are provided in Table 2. (b) The fitted lines to the experimental data (circles) for the Pu(III) aqua ion are based upon the direct proportionality of i_p with $\nu^{1/2}$, according to the diffusion model.

Figure 5), indicating quasireversible behaviors essentially free from complications associated with reactivity of the electrolyzed analyte. For the Pu(III) aqua ion, the significantly larger deviation from unity for the corresponding average ratio (1.29, Table 2) and its variation with the scan rate (see the Supporting Information, Figure 5) reflect the influence of complicating behaviors from, for example, effects of chemical instabilities, such as disproportionation. For the Pu(III) aqua ion, the ΔE_p values exhibit a slight, direct dependence on the scan rate (see Table 1, wave I′), with an average value of 64 ± 4 mV that is consistent with a one-electron Pu(III)/Pu(IV) processes at 25 °C.[37] As expected, the average value of ΔE_p for the equivalent process in $[PuPA]^{12-}$ is the same (65 mV, see Table 1). However, the associated standard deviation is substantial (±30 mV), reflecting the direct dependence on the scan rate (see Table 1, wave I′, and Supporting Information, Figure 6).

Discussion

The Na^+ exchange reaction with Pu(IV) was envisioned to proceed in similar fashion to the parallel reactions with Th(IV) and U(IV),[23,33,38] and according eq 1.

$$[NaPA]^{14-} + Pu(IV) \rightarrow [Pu(IV)PA]^{11-} + Na^+ \quad (1)$$

At the high acidity of the aqueous exchange medium, 0.525 M $[H^+]$, the disproportionation of Pu(IV) according to eq 2 is a facile process.[41]

$$3Pu(IV) \rightarrow 2Pu(III) + Pu(VI) \quad (2)$$

The observation of the plutonyl(VI) optical spectrum for the mother liquor, Figure 2a, and the incorporation of Pu(III) in the Preyssler anion are strong indicators that disproportionation precedes the exchange reaction, eq 3.

$$[NaPA]^{14-} + Pu(III) \rightarrow [Pu(III)PA]^{12-} + Na^+ \quad (3)$$

In support of this line of evidence from the preparative chemistry with Pu(IV), the reaction of Np(IV) with $[NaPA]^{14-}$, under hydrothermal conditions that yield $[PuPA]^{12-}$, does not lead to the encapsulation of neptunium. Unlike Pu(IV), Np(IV) is not prone to disproportionation (as the potentials in the Latimer diagram indicate)[42] but, rather, susceptible to one-electron oxidation according to eq 4:

$$Np(IV) \rightarrow [Np(V)O_2]^+ \quad E^\circ = +0.57\ V \quad (4)$$

The Np(IV) reaction with $[NaPA]^{14-}$, which is a multielectron oxidant, produces the neptunyl(V)−$[NpO_2]^+$−aqua ion, which is a stable species in aqueous mineral acid media,[32] and the original $[NaPA]^{14-}$ (see Supporting Information, Figure 1). No exchange takes place, not even for $[NpO_2]^+$, despite what appears to be ideal accommodations for the linear *trans*-dioxo cation within the tunnel, and the original Preyssler anion is recovered quantitatively. Although the cylindrical cavity through the P−W−O framework structure, Figure 1, appears tailor-made for an $[O{=}Np{=}O]^+$ moiety, steric effects may prohibit its exchange with Na^+ and its subsequent encapsulation.

Whereas the U(IV)-exchange reaction with $[NaPA]^{14-}$ exhibits sensitivities to experimental conditions, U(IV) can be encapsulated when its two-electron oxidation reaction of eq 5 is suppressed by control of the pH.

$$U(IV) \rightarrow [U(VI)O_2]^{2+} \quad E^\circ = +0.27\ V \quad (5)$$

Because the standard electrode potentials indicate that Np(IV) is more stable to oxidation than U(IV), it is possible that the Np(IV)-exchange reaction could be achieved through judicious variations of pH or, alternatively, with Np(III) instead, and requiring conditions and physical controls other than conventional hydrothermal ones, including nonaqueous systems. From collective experimentation with tetravalent-

(42) Morss, L. R. In *Handbook on the Physics and Chemistry of Rare Earths*; Gschneidner, K. A., Jr., Eyring, L., Choppin, G. R., Lander, G. H., Eds.; Elsevier Science: Amsterdam, 1994; Vol. *18*, pp 239−291.

and trivalent-actinide ion exchange chemistry,[23,29,33,38] including that for plutonium given in this report, wherein Preyssler anions containing all of the customary actinides except Np (including Th(IV), U(IV), Pu(III), Am(III), and Cm(III)) have been prepared and characterized, it follows that Np redox chemistry, and not ionic size, is the pivotal issue preventing the exchange of either Np(IV) or Np(III) with Na^+ in $[NaPA]^{14-}$.

Previous work has shown that cations, M, of various charges, $1 \leq n \leq 4$, with ionic radii (IR) of 1.09−1.36 Å, inclusive (for CN = X),[43] form $[MPA]^{n-15}$ molecular anions.[29] The IR of Pu(III), 1.24 Å as extrapolated from the compilation of Shannon,[43] is between those for Ca(II), 1.23 Å, and Ce(III), 1.25 Å, which readily form $[CaPA]^{13-}$ and $[CePA]^{12-}$. From the perspective of IR arguments, the encapsulation of Pu(III) is in line with known exchange chemistry. What is unique about the $[PuPA]^{12-}$ system is that the encapsulated Pu(III) is electroactive—oxidizable to Pu(IV) as $[PuPA]^{11-}$ and reversibly reduced to the as-prepared form—at a potential that is 1.077 V more positive than the first reduction couple (I) of the P−W−O framework. In accordance with interpretations of phthalocyanine[44] and porphyrin[45] redox chemistry, the difference between the $E_{1/2}$ values for the first reduction (I, −0.117 V) and the first oxidation (I′, +0.960 V) provides an electrochemical measure of the HOMO−LUMO energy gap in the system. This value, 1.077 V, which is equivalent to 1151 nm, compares favorably with those of 1.7−1.9 V calculated for Preyssler anions encapsulating Na^+, Ca(II), La(III), and Th(IV).[27,34] In addition, the low-energy, NIR features noted in Figure 2b between the bands at 1099 and 1168 nm (corresponding to 1.128 and 1.062 V, respectively) provide an independent gauge of the HOMO−LUMO gap.

The $E_{1/2}$ value (+0.960 V) for the Pu(III)/Pu(IV) couple, I′, is 0.197 V greater than $E_{1/2}$ (+0.763 V) for the corresponding couple of the Pu(III) aqua ion. This indicates that a moderate stabilization of the Pu(III) ion is achieved by encapsulation, consistent with the qualitatively similar effects noted previously for Ce(III) and Eu(II).[14,20] The quantitative voltage difference accessible with the $[PuPA]^{12-}$ system is defensible, more so than those estimated from electroanalytical measurements made on the $[CePA]^{12-}$ and $[EuPA]^{12-}$ systems. In the former case, the Ce(III)/Ce(IV) couple cannot be observed within the aqueous polarization window afforded by aqueous electrolytes, and[14] in the latter, the Eu(III)/Eu(II) couple is strongly correlated with the addition of electrons to the W−O LUMO, resulting in a nonlinear Nernst plot and uncertainty in the formal electrode potential.[22] Nevertheless, the more positive $E_{1/2}$ value for the Pu(III)/Pu(IV) couple in the $[PuPA]^{12-}$ complex in comparison to that for the cationic Pu(III) aqua species is unusual but not without precedence. Electrochemical data obtained for Eu(III) cryptate complexes, $Eu[2.2.1](NO_3)_3$ and $Eu[2.2.2](NO_3)_3$, reveal that the Eu(III)/Eu(II) couple is more positive than that for the reduction of the cryptand-free Eu(III) aqua ion.[30] Moreover, the electrode processes for $[Pu(III)PA]^{12-}$ and the Pu(III) aqua ion, both in 1 M HCl, exhibit contrasting behaviors. On the one hand, the anodic and cathodic peak currents for the Pu(III)/Pu(IV) couple in $[Pu(III)PA]^{12-}$ are proportional to the scan rate, consistent with nernstian, surface-confined behavior. On the other, the peak currents for the Pu(III) aqua ion show a linear response with the square root of the scan rate, which is indicative of nernstian waves for mass-transport-controlled diffusion behavior. Insight into this behavior can be obtained by comparisons of the Pu(III) and Pu(IV) coordination environments in $[PuPA]^{12-/11-}$.

The IR of Pu(IV), 1.06 Å as extrapolated from the results by Shannon,[43] is essentially the same as that of Ce(IV), 1.07 Å, which does not form an exchange product with the Preyssler anion, and smaller than that for U(IV), 1.09 Å, heretofore the smallest encapsulated cation.[29] Previous studies of the M^{n+} environments in $[M^{n+}PA]^{n-15}$ by the use of single-crystal XRD[25,26] and EXAFS[29,46] show that all M^{n+}'s are confined within the tunnel-like cavity running through the anion by 10 O atoms that form the inside surface, see Figure 1. In view of the structural rigidity of the host, there is no slack, conformational flexibility available within the void space to accommodate the bonding requirements of various M^{n+} ions precisely. Much like the rigid tunnel voids connecting cages in zeolite structures, the fixed tunnel size of the Preyssler anion cannot accommodate all M^{n+}'s with equal ease. The only variation possible is for the guest cation to translate along the central C_5 axis of the anion, and this is exactly what occurs. Small M^{n+} ions, such as Pu(IV), reside near the top of the anion, whereas larger ones, like Pu(III), are deeper down. Despite the 0.18 Å difference in IR between Pu(III) and Pu(IV), the average $Pu-O_{10}$ distances are calculated to be essentially the same, 2.66 and 2.63 Å, respectively,[47] indicating that the valence-driven movement of Pu along the C_5 axis through the tunnel is much less than the IR difference.[29] As such, the small Pu−O distance difference, 0.03 Å, is not accommodating for the Pu(IV) ion, which is coordinatively undersaturated within the tunnel,[48] and the likely source for the greater difficulty (more positive electrode potential) of oxidation of Pu(III) in $[PuPA]^{12-}$ than for the oxidation of the Pu(III) aqua ion. Most importantly, the fact that Pu(III) is surface bound within the Preyssler anion and that the Pu(III) aqua ion is a freely diffusing species accounts for the difference in electron

(43) Shannon, R. D. *Acta Crystallogr.* **1976**, *A32*, 751–767.
(44) Li, R.; Zhang, X.; Zhu, P.; Ng, D. K. P.; Kobayashi, N.; Jiang, J. *Inorg. Chem.* **2006**, *45*, 2327–2334.
(45) Kadish, K. M.; Van Caemelbecke, E.; Royal, G. In *The Porphyrin Handbook*; Kadish, K. M., Smith, K., Guilard, R., Eds.; Academic Press: San Diego, CA, 2000; Vol. *8*, pp 1−114.
(46) Williams, C. W.; Antonio, M. R.; Soderholm, L. *J. Alloys Compd.* **2000**, *303−304*, 509–513.
(47) The positions of Pu(III) and Pu(IV) were arithmetically modeled according to the procedure described beforehand,[29] wherein R_1 is defined as the Pu distance to the five O atoms of the outer O pentagon (O_5-1) and R_2 is defined as the Pu distance to the five O atoms of the inner O pentagon (O_5-2). The R_1 and R_2 values for $[Pu(III)PA]^{12-}$ are 2.64 and 2.68 Å, respectively, and the average $Pu(III)-O_{10}$ distance is 2.66 Å. The corresponding values for $[Pu(IV)PA]^{11-}$ change to 2.46 and 2.79 Å, respectively, with an average value of 2.63 Å.
(48) BVS calculations for the arithmetically modeled $Pu(III)-O_{10}$ and $Pu(IV)-O_{10}$ distances in $[Pu(III)PA]^{12-}$ and $[Pu(IV)PA]^{11-}$ provide values of 2.52 and 2.81, respectively, indicating that the tunnel cavity through the Preyssler anion favors the encapsulation of trivalent Pu over tetravalent Pu.

transfer kinetics, wherein the Pu(III)/Pu(IV) couples exhibit electrochemical parameters consistent with surface-confined behavior for the cluster anion and mass-transport-controlled behavior for the free cation.

With the information in hand for the $[PuPA]^{12-}$ system, insights into the behavior of the $[CePA]^{12-}$ system can be brought to light. Both experimental and theoretical studies indicate that the preparation of $[Ce(IV)PA]^{11-}$ in aqueous media is not possible.[14,27] The issue is not one of ionic size—Ce(IV) and Pu(IV) have essentially equivalent IRs—but because of the Ce(III)/Ce(IV) redox chemistry. The thermodynamic electrode potential for the oxidation of the free Ce(III) aqua ion in acidic media is very positive, +1.52 V.[12] This value is 0.714 V greater than that for the equivalent Pu couple. The additional stabilization of ca. +0.20 V, equivalent to the value obtained here for $[Pu(III)PA]^{12-}$ (Figure 5), of the large Ce(III) ion in $[CePA]^{12-}$ pushes the electrode potential at which the Ce(III)/Ce(IV) couple would be observed to even more positive values, which are well beyond the accessible domain of aqueous electroanalytical chemistry.

Conclusions

The *trans*-uranium POM chemistry of the Preyssler anion has been expanded to include the preparation of the Pu(III)-exchanged complex, $[PuP_5W_{30}O_{110}]^{12-}$, which combines an electroactive actinide within the framework of an electroactive complexant in a single heterobinuclear molecular anion. The two redox-active centers involve valence orbitals of dissimilar character—localized 5f states of Pu and 5d-band states of W—and dual redox activity is demonstrated wherein the Pu(III)/Pu(IV) couple occurs at an electrode potential that is 1.077 V above the onset of the multielectron reductive electrochemistry of W(VI) in the P−W−O anion, leading to the formation of a heteropoly blue species. The electrode potential for the Pu(III)/Pu(IV) couple in $[PuPA]^{12-}$ is 0.20 V more positive than that for the Pu(III) aqua ion, indicating the stabilization of Pu(III) by its encapsulation in the Preyssler anion. The rigid $Pu-O_{10}$ coordination environment provided by the O atoms that form the inside surface of the Preyssler tunnel is more favorable for Pu(III) bonding than for Pu(IV) bonding. The fact that the encapsulated Pu is not directly exposed to the electrolyte medium and, moreover, cannot come into direct contact with the electrode surface accounts for differences in Pu(III)/Pu(IV) electron-transfer kinetics between $[Pu(III)PA]^{12-}$ and the Pu(III) aqua ion. Preparative difficulties regarding the redox stabilization of the monatomic spherical cations of Np(IV) and Np(III) have prevented the exchange of Np with Na^+ in $[NaPA]^{14-}$, which has also shown no indication for the encapsulation of the triatomic, linear, *trans*-dioxo neptunyl(V) cation under standard hydrothermal conditions, despite what may look like a favorable host−guest match in terms of stereochemistry.

Acknowledgment. We thank Clayton W. Williams and L. Soderholm (ANL) for assistance during the initial stages of this work, which was supported by the U.S. Department of Energy, Office of Basic Energy Science, Division of Chemical Sciences, Biosciences and Geosciences, under contract No DE-AC02-06CH11357.

Supporting Information Available: Figures 1−6 containing details obtained from scan-rate-dependent cyclic voltammetry experiments. This material is available free of charge via the Internet at http://pubs.acs.org.

IC8008893